

VARIOUS EFFECTS OF GALAXY FLYBYS: DEPENDENCE ON IMPACT PARAMETER

A. MITRAŠINOVIĆ^{1,3}, M. MIĆIĆ¹, M. SMOLE¹, N. STOJKOVIĆ^{1,3}, N. MARTINOVIĆ²
and S. MILOŠEVIĆ³

¹*Astronomical Observatory, Volgina 7, 11060 Belgrade, Serbia*
E-mail: amitrasinovic@aob.rs

²*Mathematical Institute of the Serbian Academy of Sciences and Arts,
Kneza Mihaila 36, 11000 Belgrade, Serbia*

³*Department of Astronomy, Faculty of Mathematics,
Studentski trg 16, 11000 Belgrade, Serbia*

Abstract. Galaxy flybys, interactions where two independent halos inter-penetrate but detach at a later time and do not merge, occur frequently at lower redshifts. Due to their violent nature, these interactions can significantly impact evolution of individual galaxies - from mass loss, and shape transformation, to emergence of tidal features, and formation of morphological disc structures (e.g. bar, spiral arms).

Based on N-body simulations of galaxy flybys, these various effects will be discussed briefly in the context of different impact parameters. While there is clear dependence on impact parameter for some effects, results suggest that secular evolution of galaxies should not be neglected.

1. INTRODUCTION

Galaxy flyby, as defined here, is an interaction where two independent halos inter-penetrate but detach at a later time, thus not resulting in a merger. It has to be noted that these interactions should not be mistaken for close galaxy passages where two halos remain separate at all times. Based on the analysis of cosmological N-body simulations, Sinha & Holley-Bockelmann (2012) found that this type of interaction can be as frequent as mergers. The number of flybys is comparable to the number of mergers on high redshift ($z > \sim 14$), while it can even surpass the number of mergers on lower redshifts ($z < \sim 2$) for halo masses $> \sim 10^{11} M_{\odot} h^{-1}$. In the second part of the series (Sinha & Holley-Bockelmann 2015), the authors further explored parameters of flybys and found that, in majority of flybys, secondary halo penetrates deeper than $\sim R_{\text{half}}$ with initial relative velocity $\sim 1.6 \times V_{\text{vir}}$ of the primary halo. Typical flyby mass ratio was found to be ~ 0.1 at high redshifts, or lower, at the lower redshift end. While major flybys (with mass ratio greater than 0.3 or even close to 1) are still possible, they are extremely rare.

Both frequency and strength of galaxy flybys suggest that these interactions have a potential to significantly impact evolution of individual galaxies. Previous studies, however scarce, explored various effects of galaxy flybys, primarily focusing on pri-

mary, more massive galaxy. Kim et al. (2014) showed that flybys can create warps at the edges of primary galaxy disk, visible in both gaseous and stellar component. Lang et al. (2014) examined the role of galaxy flybys in bar formation. They found that bar forms in both galaxies in flybys with mass ratio 1, and only in secondary with mass ratio 0.1. They also noted that induced changes are significantly stronger in flybys with prograde¹ orbits (as opposed to retrograde orbits). This was later additionally examined in more detail, and confirmed by Lokas (2018). Detailed study accounting for different galaxy models and orbits (flybys with different mass ratios and different strength of interaction) was done by Pettitt & Wadsley (2018). The authors covered a broad range of initial conditions and found that diverse morphological features can emerge - bars of various strengths and lengths and various manifestations of spiral structure. Particularly of interest is new critical condition for strength of interaction: the authors found that morphological features can emerge in much weaker interactions than previously known. Despite the lack of detailed studies examining secondary galaxy, flybys could still be as significant for its evolution. They were discussed briefly as a potential contributor to formation of ultra-diffuse galaxies (Wright et al. 2020).

The main goal of our work is to probe impact parameter and investigate its role in deeper flybys (where secondary halo penetrates deeper than half mass radius of the primary halo, R_{half}). This approach aims to answer a question: is there a functional dependence on impact parameter for these various effects, and if so - what does it look like? In the following sections, we will describe our models, methods and simulations and give a brief overview of preliminary results.

2. METHODS

Primary galaxy model, with virial radius $R_{\text{vir}} = 197.4$ kpc, was constructed as three-component model consisting of: NFW dark matter halo (600.000 particles with total mass $M_H = 9.057 \cdot 10^{11} M_\odot$), exponential stellar disk (300.000 particles with total mass $M_D = 7.604 \cdot 10^{10} M_\odot$), and Sérsic stellar bulge (100.000 particles with total mass $M_B = 2.502 \cdot 10^{10} M_\odot$). For the sake of simplicity, intruder galaxy, with virial radius $R_{\text{vir}} = 91.56$ kpc, was scaled down to be 10 times smaller (in both number of particles and total mass), and consisting only of spherical components: NFW dark matter halo (60.000 particles) with total mass $M_H = 9.044 \cdot 10^{10} M_\odot$, and Sérsic stellar bulge (40.000 particles with total mass $M_S = 1.022 \cdot 10^{10} M_\odot$). Both models were evolved for 5 Gyr in isolation using publicly available code **Gadget2** (Springel 2005). This was done to ensure model stability in isolation, and to provide fiducial (data) points which will help differentiate flyby-induced changes from the ones arising from secular evolution.

Flyby simulations were evolved for 5 Gyr with outputs (snapshots) being saved every 0.01 Gyr. Primary and intruder galaxy were set as almost contact system (initial distance being roughly equal to the sum of their virial radii, $d \simeq 290$ kpc), with primary galaxy remaining static at the center of simulation box. Intruder galaxy was set on prograde parabolic orbit coplanar with primary galaxy disk with initial relative velocity $v_0 = 500$ km s⁻¹. This value, despite being larger than the most common one, falls into the range of realistic relative velocities in galaxy flybys. By

¹the spin of the galaxy disk and its orbital angular momentum with respect to the perturber are aligned

Table 1: List of flyby simulations where b is pericentre distance (impact parameter), $R_{\text{vir},1}$ virial radius of main galaxy, and v_b pericentre velocity.

Name	b [kpc]	$b/R_{\text{vir},1}$	v_b [km s $^{-1}$]
B30	22.50	0.114	660.14
B35	26.53	0.135	650.86
B40	30.69	0.156	641.80
B45	35.07	0.178	632.86
B50	39.62	0.201	624.25
B55	44.27	0.224	616.16
B60	48.99	0.248	608.09
B65	53.72	0.272	601.28

slightly varying angles of initial position and intruder velocity vector, we achieved different impact parameters in different simulations while keeping interaction duration constant at 1.08 Gyr. Interaction duration is defined as the time during which halos overlap, i.e. distance between centers of galaxies is smaller than the sum of their virial radii, $d \leq R_{\text{vir},1} + R_{\text{vir},2}$. List of flyby simulations with relevant parameters is given in Table 1.

2. 1. ANALYSIS PROCEDURES

Our method is based on Fourier analysis for detection of morphological structures (bars and two armed spirals) in primary galaxy disk. When disk is decomposed in Fourier modes, these structures contribute the most to second mode C_2 . Relative (mass normalized, since zeroth mode C_0 yields total mass) second mode is calculated as:

$$\frac{C_2}{C_0} = \frac{1}{M} \sum_{j=1}^N m_j e^{2i\phi_j} = C_{21} + iC_{22} \quad (1)$$

where M is total mass, and summation is performed over all particles with masses m_j and angles ϕ_j in $x - y$ plane. We then calculate amplitude $A_2 = \sqrt{C_{21}^2 + C_{22}^2}$ and phase $\phi_2 = \arctan(C_{22}/C_{21})$. Calculation was performed locally, by slicing the disk in annuli in $x - y$ plane for each simulation snapshot. This results in evolution maps for both amplitude $A_2(t, R/R_D)$ and phase $\phi_2(t, R/R_D)$ where R is central radius of each annulus, R_D disk scale radius, and t time of each snapshot. Detailed analysis is out of scope of this article, yet these maps can provide serviceable insight into structure formation and evolution. Both stellar bars and two armed spiral structure are characterized by high enough amplitude A_2 (most commonly $A_2 > 0.2$) but they differ in behaviour of phase ϕ_2 along radial component - bars have almost constant phase while phase of spiral arms is uniformly changing.

While analyzing intruder galaxy, we used three different mass estimates which we will refer to as: bound, virial and core mass. Bound mass filters particles with negative total energies (sum of kinetic and potential energy), thus gravitationally bound particles. Virial mass filters particles inside virial radius, which was determined by fitting NFW to spherical density profile, for each snapshot. Finally, core mass estimate is based on circular velocity profile. First, we calculate circular velocity

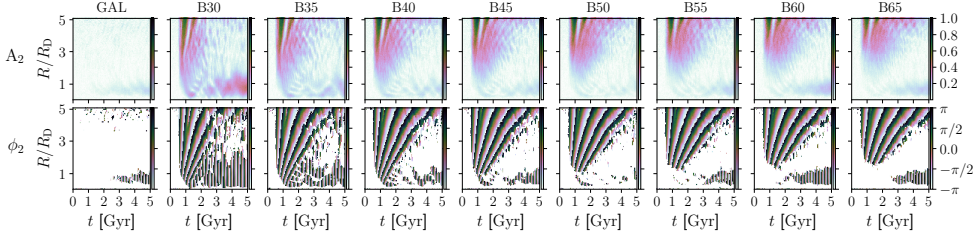


Figure 1: Evolution maps of Fourier second mode: amplitude $A_2(t, R/R_D)$ (upper panels) and phase $\phi_2(t, R/R_D)$ (lower panels). GAL row shows primary galaxy fiducial simulation, while the rest are showing flyby simulations, as defined in Table 1.

profile as $V_{\text{circ}}(r) = \sqrt{GM(< r)/r}$, where $M(< r)$ is cumulative mass and r spherical radius. Radius r_{\max} where this profile reaches maximum V_{\max} is chosen as cutoff, and $M(< r_{\max})$ represents core mass.

3. RESULTS

3. 1. PRIMARY GALAXY

Fourier maps described in previous section are shown on Figure 1: amplitude $A_2(t, R/R_D)$ (upper panels) and phase $\phi_2(t, R/R_D)$ (lower panels). GAL row shows primary galaxy fiducial simulation, while the rest are showing flyby simulations, as defined in Table 1.

Two armed spiral structure forms almost immediately after the interaction. Radii of origin appear directly proportional to impact parameter, starting lower than scale radius ($R/R_D < 1$) in simulation with the lowest impact parameter (B30), and ending with mid-disk origin ($R/R_D \geq 2$) in simulation with the highest impact parameter (B65). However, these *deeper* spiral arms tend to wind up and dissolve faster suggesting that their lifetimes are inversely proportional to impact parameter.

Early bar formation is observed in two closest simulations (B30, B35). In B30, formed bar quickly evolves to get stronger and longer and remains present until the end of simulation, while its evolution in B35 is slower and chaotic. Bar evolution gets more stable in simulations with larger impact parameters, but their strengths and lengths do not correlate uniformly with impact parameter. One of the simulations (B50) is particularly interesting due to suppression of pre-existing bar instability (i.e. that the bar never fully forms). One possible explanation for chaotic bar evolution (in simulations with lower impact parameters) is co-evolution with winded, dissolving spiral arms. Spiral structure's and bar's regions never overlap in B55, b60, and B65 - allowing independent evolution of these features. This does not explain non-uniform dependence of bar's strength and length with impact parameter - more detailed analysis is needed to tackle that issue.

3. 2. INTRUDER GALAXY

Stellar component of intruder galaxy retains its mass, while significant dark matter mass loss is observed. Evolution of mass estimates is shown on Figure 2. Bound mass

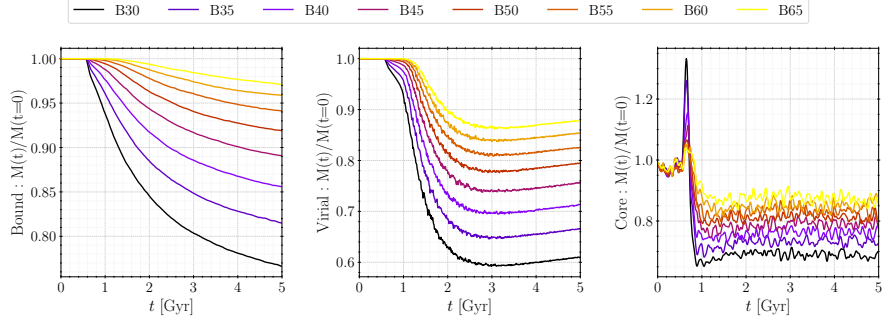


Figure 2: Evolution of mass estimates: bound mass (left), virial mass (middle), and core mass (right panel). Different simulations are represented with different colors. All mass estimates are calculated as a fraction of initial mass.

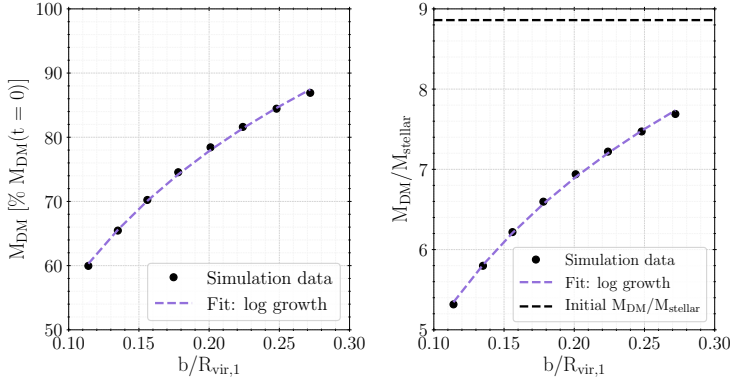


Figure 3: *Left:* Average virial mass of dark matter component after 2.5 Gyr (as a percentage of initial virial mass) as a function of impact parameter (in units of primary galaxy virial radius). Dots represent different simulations, while dashed line shows log growth fit. *Right:* Similarly to left panel, dark-to-stellar mass ratio after 2/5 Gyr as a function of impact parameter. Additional black dashed line represents initial dark-to stellar mass ratio.

continually decays until the end of every simulation. This is due to definition of this estimate - it includes gravitationally bound tidal features which, eventually unbind and detach from intruder galaxy. Core mass stabilizes by the end of interaction, being fairly constant with negligible variations until the end of every simulation. Core mass loss is lower than virial mass loss, implying that the core of intruder is semi-preserved. Following steep decline, virial mass stabilizes after 2.5 Gyr. Due to recapturing of some particles forming tidal feature, virial mass slightly increases near the end. Nevertheless, this mass estimate provides the best insight into total intruder mass. Thus, average virial mass after 2.5 Gyr is used in further analysis. It is shown on Figure 3 as a function of impact parameter, alongside dark-to-stellar mass ratio. Logarithmic growth (with impact parameter) for both of these is evident.

4. SUMMARY

Galaxy flyby is an interaction where two independent halos inter-penetrate but detach at a later time and do not merge. We performed a series of simulations to explore dependence of various effects caused by these interactions on impact parameter.

Both two armed spirals and stellar bars can form in the disk of primary galaxy. Spiral arms show clear dependence on impact parameter - their radii of origin are directly and their lifetimes are inversely proportional to impact parameter. Stellar bars, however, have non-uniform dependence on impact parameter. Strong and long bar forms in simulation with the smallest impact parameter, followed by weaker bar with chaotic evolution as impact parameter increases. Bar evolution gets more stable towards the highest impact parameters, but its strengths and lengths do not correlate with impact parameter. Suppression of pre-existing bar instability is also detected in one of the simulations. All of this raises new questions - did we neglect other possible contributions to chaotic bar evolution, and should we consider co-evolution of stellar bars and spiral arms?

We also found that secondary, intruder galaxy exhibits significant dark matter mass loss, while stellar component remains unaffected. This translates to decrease in dark-to-stellar mass ratio. Dependence of both virial mass and dark-to-stellar mass ratio on impact parameter follows logarithmic growth law. It is unclear whether this logarithmic growth law is universal or sensitive to initial conditions. Most likely, the law itself should remain universal with possible different fitting parameters for different initial conditions. This result is particularly of interest as it suggests that strongest or multiple subsequent flybys have the potential of stripping intruder galaxy of majority of its dark matter. More research is needed to fully explore those possibilities.

Acknowledgements

This work was supported by the Ministry of Education, Science and Technological Development of the Republic of Serbia (MESTDRS) through the contract no. 451-03-68/2020/14/200002 made with Astronomical Observatory of Belgrade, and the contract no. 451-03-68/2020/14/200104 made with Faculty of Mathematics, University of Belgrade.

References

- Kim, J. H., Peirani, S., Kim S., Ann, H. B., An, S.-H., Yoon, S.-J.: 2014, *The Astrophysical Journal*, **789**, 90.
- Lang, M., Holley-Bockelmann, K., Sinha, M.: 2014, *The Astrophysical Journal Letters*, **790**, L33.
- Lokas, E. L.: 2018, *The Astrophysical Journal*, **857**, 6.
- Pettitt, A. R., Wadsley, J. W.: 2018, *Monthly Notices of the Royal Astronomical Society*, **474**, 5645.
- Sinha, M., Holley-Bockelmann, K.: 2012, *The Astrophysical Journal*, **751**, 17.
- Sinha, M., Holley-Bockelmann, K.: 2015, *arXiv e-prints*, arXiv:1505.07910.
- Springel, V.: 2005, *Monthly Notices of the Royal Astronomical Society*, **364**, 1105.
- Wright, A. C., Tremmel, M., Brooks, A. M., Munshi, F., Nagai, D., Sharma, R. S., Quinn, T. R.: 2020, *arXiv e-prints*, arXiv:2005.07634.